AD-A096 887 CORNELL UNIV ITHACA N Y DEPT OF MATERIALS SCIENCE A--ETC F/G 11/2
DEFORMATION OF AMORPHOUS FE40NI40P14B6 UNDER COMPRESSION TO 250--ETC(U)
MAR 81 H KIMURA, D G AST, W A BASSETT N00014-77-C-0546
UNCLASSIFIED TR-5 NL

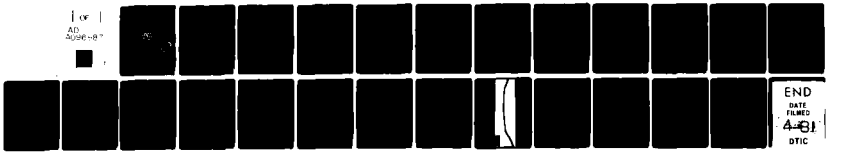

SECURITY CLASSIFICATION OF THIS PAGE (When Data Entered)

REPORT DOCUMENTATION PAGE

READ INSTRUCTIONS BEFORE COMPLETING FORM

1. REPORT NUMBER: Technical Report No. 5
2. GOVT ACCESSION NO.: AD-A096 887
3. RECIPIENT'S CATALOG NUMBER:

4. TITLE (and Subtitle): Deformation of Amorphous $Fe_{40}^{\Pi}Ni_{40}^{\Pi}P_{14}^{\Pi}B_{6}^{\Pi}$ under Compression to 250 Kbar.
5. TYPE OF REPORT & PERIOD COVERED: 12/15
6. PERFORMING ORG. REPORT NUMBER:

7. AUTHOR(s): H./Kimura, D. G./Ast, W. A./Bassett
CONTRACT OR GRANT NUMBER: NR 039-151, N00014-77-C-0546

9. PERFORMING ORGANIZATION NAME AND ADDRESS: Dept. of Materials Science & Engineering, Bard Hall, Cornell University, Ithaca, NY 14853
10. PROGRAM ELEMENT, PROJECT, TASK AREA & WORK UNIT NUMBERS: 11, 2 Mi

11. CONTROLLING OFFICE NAME AND ADDRESS: 14, TR-5
Metallurgical Branch, ONR, Arlington, VA 22217
12. REPORT DATE: 3/5/81
13. NUMBER OF PAGES: 22

14. MONITORING AGENCY NAME & ADDRESS(if different from Controlling Office): 15 NR 114-77-C-0546, WSF-EAF 79-19972
15. SECURITY CLASS. (of this report):
15a. DECLASSIFICATION/DOWNGRADING SCHEDULE:

LEVEL II

16. DISTRIBUTION STATEMENT (of this Report): Unlimited

DISTRIBUTION STATEMENT A
Approved for public release; Distribution Unlimited

17. DISTRIBUTION STATEMENT (of the abstract entered in Block 20, if different from Report)

DTIC ELECTE MAR 24 1981 S C

18. SUPPLEMENTARY NOTES

19. KEY WORDS (Continue on reverse side if necessary and identify by block number)

Metallic glass, high pressure, work softening, free volume, stick-slip transition

20. ABSTRACT (Continue on reverse side if necessary and identify by block number)

Metallic glass was compressed in the diamond cell to 250 kbar and the pressure was measured as a function of position with the ruby method. Analysis of P(r) yields a flow stress of 17 kbar, and pressure dependence of 0.4% per kbar. The pressure dependence is similar to that of crystalline Fe.

DD FORM 1 JAN 73 1473 EDITION OF 1 NOV 65 IS OBSOLETE
S/N 0102-LF-014-6601

403 [illegible]

SECURITY CLASSIFICATION OF THIS PAGE (When Data Entered)

AD A096887

DTIC FILE COPY

81 3 23 007

Deformation of Amorphous $Fe_{40}Ni_{40}P_{14}B_6$ under Compression to 250 Kbar

H. Kimura[+]

D.G. Ast[+]

W.A. Bassett[++]

+) Department of Materials Science and Engineering, Bard Hall, Cornell University

++) Department of Geological Sciences, Kimball Hall, Cornell University

ABSTRACT

Amorphous $Fe_{40}Ni_{40}P_{14}B_6$ was compressed in the diamond anvil cell up to 250 kbar pressure and the pressure was measured as a function of position with the ruby fluorescence method.

The pressure distribution indicates that the flow stress, σ_y, of the material under pressure is 17 ± 1 kbar ($\sim$173 kg/mm^2). The pressure dependence of the flow stress is about 0.4 ± 0.1% per 1 kbar of hydrostatic pressure.

The value of the flow stress under pressure is about 30% smaller than the flow stress at zero pressure. The decrease in flow stress is ascribed to work-softening, and a work softening coefficient $d\sigma/d\varepsilon \lesssim 1.5$ is derived.

1) Introduction

The flow stress of metallic glasses under high pressure is of interest, since the pressure dependence of the flow stress makes it possible, in principle, to discriminate between the various theoretical models for plastic flow in glassy metals.

The first measurement of the influence of hydrostatic pressure on flow was carried out by Davis and Kavesh,[1] who measured the yield stress in compression of $Pd_{77.5}Cu_6Si_{16.5}$ at hydrostatic pressures up to 6.2 kbar. The pressure dependence of the yield stress was found to be quite small, about 0.5% per kilobar of applied pressure, which is comparable to the pressure dependence of crystalline metals. Because the pressure dependence of the elastic constants of amorphous metals is not known, no firm conclusions could be drawn as to which theoretical model would best fit the data.

Very much higher pressures can be applied in the diamond anvil press. At 250 kbar, a value which is relatively easily achieved without undue risk of fracturing the diamonds, the applied stress exceeds the yield stress of a metallic glass by more than one order of magnitude. The material flows in a semi-fluid like fashion and extensive plastic flow, with strain of 20% or more, occurs without fracturing or separating the material.

The ability to study the influence of large plastic strains on the mechanical behavior of macroscopically brittle materials is an important advantage of the diamond cell.

In this paper we report i) the pressure distribution of an Fe-Ni based metallic glass compressed in the diamond anvil cell and ii) the analysis used to derive from the measured pressure distribution the yield stress and it's pressure dependence.

2) Theoretical pressure distribution

The homogeneous compression of a thin disc between infinitely stiff plates is discussed, e.g., by Polakowski and Ripling,[2] under the assumption that the flow stress does not depend on pressure. The pressure distribution is derived from a consideration of the equilibrium between the frictional forces at the specimen-anvil interface and the gradient of the radial stress in the specimen, σ_r. In polar coordinates, (see Fig. 1) with z perpendicular to the plane of the disc, the forces on a differential element of the disc of dimension $h.dr.r.d\phi$, where h is the disc thickness, balance each other if:

$$d\sigma_r.h. = 2.dr.F \qquad (1)$$

F is the friction force per unit area. The factor two takes into account that friction occurs both at the top and the bottom surface.

At low pressures, the friction force is given by Coulombs friction law as:

$$F = \mu.P_z \qquad (2)$$

where μ is the coefficient of friction and P_z is the normal stress on the disc surface. A typical value for μ for a crystalline metal, in contact with a hard unlubricated surface would be 0.15.[3]

Equation (2) is valid only if the friction force F is lower than the critical shear stress τ_c of the material being tested. For $F \geq \tau_c$, the material deforms by "smearing". The condition is also known as sticking, since there is no relative movement at the specimen-anvil interface. Transition from sliding to smearing occurs at a critical value P_z':

$$P_z' = \tau_c/\mu \qquad (3)$$

For $P_z > P_z'$, the friction force is constant and equal to τ_c. To estimate at which value of P_z this transition might occur for a metallic glass, we take $\mu = 0.15$, and assume further that the ruby particles which reside at the interface in order to measure the pressure, have no influence on the friction coefficient. τ_c is about 10 kbar, and from eq. (3) we would therefore expect P_z' to

be about 60 to 70 kbars. Above this value, equation (2) is replaced by the sticking condition:

$$F = \tau_c (P) \tag{4}$$

The notation $\tau_c(P)$ was chosen to indicate that τ_c may depend on the hydrostatic pressure P. For later, we note that P and P_z can be linked by Tresca's yield criterion:

$$P = P_z - (4/3)\tau_c(P) \tag{5}$$

In the diamond press P_z is usually much larger than τ_c, and the stress state is largely hydrostatic in nature.

We now consider the pressure distribution in more detail. For $0<P_z<\tau_c/\mu$, we obtain from equations (1) and (2):

$$d\sigma_r = (2\mu/h)P_z \, dr \tag{6}$$

Simple considerations show that $\sigma_r = \sigma_\phi$ (see ref. 2). For simplicity, we use Tresca's yield criterion to link σ_r and P_z:

$$\sigma_r = P_z - 2\tau_c(P) \tag{7}$$

We could equally well use van Mises yield criterion, in which case the critical shear stress τ_c is replaced by the critical octahedral shear stress τ_{oct}. In our case, τ_c and τ_{oct} are related by

$$\tau_{oct} = 1.1547 \cdot \tau_c \tag{8}$$

and differ therefore by ∿16%. With the aid of Eq. (5) and (7) we can rewrite Eq. (6) as a relation between P and r, i.e., the two variables measured in the experiment. For this purpose it is convenient to express the pressure dependence of $\tau_c(P)$ explicitly as:

$$\tau_c(P) = \tau_o (1 + \xi P) \tag{9}$$

where τ_o represents the critical shear stress under zero applied hydrostatic pressure and ξ the first order coefficient of τ_c. ξ is a very small number, in the order of 0.004 $kbar^{-1}$. It's physical meaning and the theory underlying e.g., (9) are discussed in section 6. Eq. (9) and (5) result in the

following first order relations between the differentials $d\sigma$, dP_z and dP:

$$dP_z = (1 + \frac{4}{3}\tau_o\xi)\ dP \tag{10}$$

$$d\sigma_r = (1 - \frac{2}{3}\tau_o\xi)\ dP \tag{11}$$

Substitution of Eq. (5), (9), and (11) into Eq. (6), and integration yields the following relation for P(r):

$$P(r) = C_1 \exp\left(\frac{2\mu r}{h(1-2\ \tau_o\xi)}\right) + C_2 \tag{12}$$

where:

$$C_1 = \frac{2}{3}\tau_o + \frac{4\tau_o}{3+4\ \tau_o\xi} \tag{13}$$

$$C_2 = -\frac{4\tau_o}{3+4\ \tau_o\xi} \tag{14}$$

Note that the hydrostatic pressure increases exponentially with distance. The constants C_1 and C_2 were calculated under the assumption that the material at the disc edge is free to expand. The bracket $(1-2\ \tau_o\xi)$ is a correction term in the order of 10%.

At higher pressures, the boundary conditions expressed by Eq. (4) applies, and Eq. (1), upon substitution of Eq. (11) can be rearranged as:

$$\frac{dP}{dr} = \frac{2\tau_o(P)}{[1 - (2/3)\ \tau_o\xi]h} \tag{15}$$

Eq. (15) reduces for the case of $\xi = 0$, i.e., a pressure independent critical shear stress to:

$$\frac{dP}{dr} = \frac{2\tau_o(P = 0)}{h} = \frac{2\tau_c}{h} \tag{16}$$

which is widely used in the analysis of high pressure experiments[4]. In crystalline and amorphous metals $\tau_o\xi \lesssim 0.05$; i.e., the first order treatment of the pressure dependence of the yield stress modifies Eq. (16) by a correction in the order of 3% which is quite small compared to other sources of error.

Equation (15) can be integrated if the functional dependence of $\tau_c(P)$ is known. The usual procedure in high pressure research is to represent $\tau_c(P)$ by the first order expansion of Eq. (9) in which case integration of Eq. (16) yields:

$$P(r) = \frac{1}{\xi}\left[\left(\exp \frac{2\tau_o \cdot \xi \cdot r}{h(1-2/3\ \tau_o \xi)}\right) - 1\right] \qquad (17)$$

A series expansion of Eq. (17) shows that P is, in the first order, linear in r, with a slope of $2\tau_o/h$:

$$P(r) = \left(\frac{2\tau_o}{h(1-2/3\ \tau_o\xi)}\right) r \left(\frac{2\tau_o}{h(1-2/3\ \tau_o\xi)}\right)^2 \frac{\xi r^2}{2} + \left(\frac{2\tau_o}{h(1-2/3\ \tau_o\xi)}\right)^3 \frac{\xi^2 \cdot r^3}{6} + \ldots \qquad (18)$$

Contrary to one's intuition, the higher order terms are, however, not negligibly small. A numerical evaluation shows, that for h = 15μ, τ_o = 10 kbar, ξ = 0.005 and a pressure P = 250 kbar, the linear term contributes 157 kbar (63%), the second order term 62 kbar (25%), the third order term 16 kbar (6%), and the remaining higher order terms 15 kbar (6%). Even the small pressure dependence of the critical shear stress of crystalline metals can, therefore, introduce noticeable curvature into P(r) of highly compressed specimen.

In the case that the critical shear stress depends exponentially (rather than linearly) on pressure; i.e.:

$$\tau(P) = \tau_o \exp(\xi P) \qquad (19)$$

one obtains, after integration:

$$P(r) = -\frac{1}{\xi} \ln\left[1 - \frac{2 \cdot \tau_o \cdot \xi \cdot r}{h(1-(2/3)\tau_o\xi)}\right] \qquad (20)$$

A series expansion of Eq. (20) shows that the functional dependence of P(r) is very similar to that of Eq. (17):

$$P(r) = \left(\frac{2\tau_o}{h(1-2/3\ \tau_o\xi)}\right)^r + \left(\frac{2\tau_o}{h(1-2/3\ \tau_o\xi)}\right)^2 \frac{\xi r^2}{2} + \left(\frac{2\tau_o}{h(1-2/3\ \tau_o\xi)}\right)^3 \frac{\xi^2 r^3}{3} + \ldots \qquad (21)$$

Note that the first two terms of Eq. (21) are identical to those in Equation (18). The difference between a linear and exponential pressure dependence is contained in the third and higher order terms.

Exponential pressure dependences of the form of Eq. 19 correspond to writing the activation energy for thermally activated flow, $\Delta G(P)$ as:

$$\Delta G(P) = \Delta G(0) - P.\Delta V \qquad (22)$$

where ΔV is the activation volume. ΔV and ξ as defined in Eq. (19) are related by:

$$\Delta V = \xi.kT \qquad (23)$$

where k is Boltzmann's constant and T the absolute temperature.

3) Experimental Procedure

The amorphous alloy $Fe_{40}Ni_{40}P_{14}B_6$ was purchased from the Allied Chemical Corporation in the form of a 25 mm wide and approximately 30 μm thick ribbon (trade name Metglass ^{R} 2826). Small sections of the ribbon were mechanically polished from both sides to a final thickness of about 20 μm. A diamond anvil cell with culet face diameters of 600 μm diameter was used to compress the specimen. Small ruby particles were positioned at the specimen diamond interface to measure the pressure distribution of the compressed specimen via the pressure induced shift of ruby R_1 fluorescence line. The observed shifts were converted to pressure using the calibration of Barnett et al.[5]:

$$P(\text{kbar}) = (\lambda - \lambda_o)\cdot 2.746 \qquad (24)$$

where λ_o is the zero pressure wavelength of the ruby R_1 line. Experimentally, the pressure can be determined to an accuracy of ± 1 kbar. The calibration expressed in Eq. (24) applies, strictly speaking, only to situations in which the pressure is purely hydrostatic. However, Eq. (24) still holds to a good approximation when the pressure is not hydrostatic, as in the present case (see ref. 4 for more details).

The pressure was measured as a function of position, by moving the cell relative to the stationary interrogating beam with the aid of two micrometers of 10 μm graduation. In a typical experiment, the pressure distribution was measured twice, first along a line through the center of the disc and then a

parallel line with an offset of 10 μm. After completion of these measurements, and release of the pressure, the specimen was mounted with cold resin and polished edgewise until it's cross section coincided with the center line along which the pressure was measured. The cross section was photographed with an optical microscope and the specimen thickness was determined from the photograph.

4) Experimental results

Fig. 2 shows the radial pressure distribution of a disc of amorphous $Fe_{40}Ni_{40}P_{14}B_6$ under an average applied pressure of about 100 kbar. The pressure increases somewhat faster than linearly with distance, as expected from theory. At very high pressures dP/dr decreases again as the pressure reaches a peak of 245 kbar. The discontinuity at 20 kbar is associated with yielding.

Fig. 3 shows the cross section of the amorphous $Fe_{40}Ni_{40}P_{14}B_6$ alloy after completion of the experiment. It can be seen that plastic flow under high pressure is macroscopically homogeneous, without the formation of cracks or voids. Etching the specimen with the same acidic solution which clearly delineates shear bands introduced by bending (see Fig. (19) in ref. 6) did not reveal any slip bands, possibly because the slip bands were too tightly spaced to be resolved by optical microscopy.

Fig. 4 shows the pressure distribution of a specimen loaded as follows: Firstly the specimen was loaded to an average applied pressure of about 20 kbar, next, the specimen was completely unloaded, and finally, the specimen was reloaded with an average applied pressure of about 50 kbar. Note that the pressure distribution above about 65 kbar is similar to that in Fig. 2, but that there is now a pronounced transition region at low pressures, in which the pressure increases only relatively slowly with distance.

5) Analysis

A problem in the analysis of the above results is that experimental curves contain both the friction controlled and sticking regimes. Although it is clear that at very high pressures sticking boundary conditions must apply, it is not obvious where the transition between the two regimes occurs. The estimate of 60 to 70 kbar in section 2 is predicated on a friction coefficient of 0.15, which is reasonable for crystalline metals in contact with hard surfaces, but does not necessarily apply to metallic glasses, decorated with small ruby particles, and sliding against diamond.

The two regimes are described by three adjustable parameters: the friction coefficient μ, the critical shear stress at zero pressure τ_o, and the pressure coefficient of the critical shear stress ξ. The range of these parameters is restricted. In particular, τ_o cannot vary greatly from the critical shear stress measured in more conventional experiments such as tension and bending[6,7]. The range of ξ is more difficult to assess, but one would be surprised if it were to deviate more than a factor three from the value measured by Davis et al on an amorphous Pd Si alloy, since the mechanical properties of the two metallic glasses are similar.

The procedure used, therefore, was to select values for τ_o and ξ within the above range in order to fit the experimental pressure distribution with Eq. (17) and (20). Two such fits, are shown in Fig. 5 and 6. Fig. 5 demonstrates that the experiment, within experimental accuracy can be fitted with τ_o = 8.5 kbar and ξ = 0.0039. Fig. 6 illustrates that a value of τ_o = 10.5 kbar, characteristic for the values obtained in conventional experiments, cannot fit the experimental data.

A corresponding analysis of Fig. 4 is difficult to carry out since the data cover a smaller load range and the sample was loaded in two steps. Attempts to fit the data with a single expression of the form of Eq. 12, 17 or 20 were unsuccessful and suggested that the data of figure 4 contain two regimes. The high pressure data $70<P<110$ kbar data can be well fitted with a straight line of slope 0.753, see Fig. 5. The data below 65 kbar can be well fitted with an exponential pressure dependence, of the form $P(r) = \tau_o \exp(\delta r)$ with an exponent δ of 0.0047, see Fig. 5. Crossover between the two fits occurs at 61 kbar. The two regimes were assumed to represent the sticking and slipping regimes, respectively. A linear fit to the data above 61 kbar corresponds to an approximation of P(r) by the leading term of the series expansion of Eq. 18 and 21. A numerical evaluation of Eq. (18) and (20) shows that the leading term, at 90 kbar, contributes about 85% to P(r). Given the restricted range of the data, an approximately linear dependence of P or r is expected, as is indeed observed. Equating the slope with the leading term in the series expansion yields a value of 8.15 kbars for τ_o.

The friction coefficient μ can be estimated both from the pressure at which the transition between the two regimes occurs and from the curvature of P(r) below 60 kbar. The transition occurs at a critical pressure $P_z' = 61$ kbar, from which, via Eq.'s (5) and (3), a value of 0.12 for the friction coefficient. An analysis of the curvature yields $\mu = 0.05$, but is, because of the small range of data, not very reliable.

6) Discussion

One may wonder, why the friction regime, if it exists at all, is so much smaller in Fig. 2. The different extent of the friction regime very likely represents the different boundary conditions at the anvil edges. Fig. 2 was obtained by loading the specimen in one step, to a peak of 250 kbar, with a reduction in thickness from 20 to 15 μm. The extruded material outside the die

exerts a residual radial stress comparable to the yield stress on the perimeter of the material under the die. The gradient in τ_r is therefore not just opposed by the friction stress but also by the residual stress on the perimeter. The situation at the edge is equivalent to the punch indentation problem for which the lower bound solution is $P_z = 4\ \tau_o$, which is twice the value of the free edge case.

The data of Fig. 4 were obtained by pre-pressing the specimen, with subsequent unloading. An outward shift of the specimen, by relaxation during the two loadings corresponds to a boundary condition which is closer to the free edge case, with a corresponding development of the friction regime.

The value of the critical shear stress measured in this experiment lies definitely below the value of 11 to 12.5 kbar measured in bending and tension (6,7). Since it is known that details of the preparation influence the yield stress of amorphous alloys, 3 specimens from the same spool from which the high pressure specimen was prepared were also tested in bending, using the method outlined in ref. 7. The average value obtained for τ_o was 11.7 kbar.

The state of the metallic glass in the diamond cell differs from the state of the material in more conventional tests in that it is both under high pressure and deformed to a very large degree. The specimen of Fig. 2 was compressed from 20 to 15 μm which corresponds to a linear strain of 20% in the z direction. It has long been suspected that extensive deformation of metallic glasses destroys the strong short range order of these materials and lowers the flow stress. The enhanced etching of shearbands has been explained with deformation induced destruction of short range order[8], and work-softening has been invoked to explain the localization of shearbands. If we ascribe the lower value of τ_o observed to work-softening, and take, for simplicity the strain in the z-direction as a

measure of the strain, the work softening coefficient $d\sigma_y/d\varepsilon \lesssim 1.4$. This value is well within the observation from bending experiments that work-softening, if it occurs, must have a work softening coefficient smaller than 2.[7]

The pressure coefficient of the critical shear stress ξ of 0.0039 has an estimated uncertainty of ± 0.001. Within experimental accuracy, the pressure coefficient of amorphous $Fe_{40}Ni_{40}P_{14}B_6$ is therefore identical to the pressure coefficient of amorphous Pd Cu Si.

It is interesting to compare the pressure dependence of amorphous $Fe_{40}Ni_{40}P_{14}B$ with the pressure dependence of crystalline metals. The pressure dependence of the flow stress in crystalline metals, at least in the well deformed state, arises mostly from the variation of the effective elastic constant, C_o, with pressure, in which case[9]:

$$\sigma_o(P) = \sigma_{oo}[1 + (C_o'/C_o)P] \tag{24}$$

where C_o' is the dimensionless pressure derivative of C_o. Note that Eq. (24) is formally identical to Eq. (9), with

$$C_o'/C_o = \xi \tag{25}$$

Which elastic constants or combination of elastic constants is to be identified with C_o depends on the mechanism controlling the flow stress and is discussed in more detail in ref. 9. Data on both C_o and C_o' are available for Fe:

$$\begin{aligned} E &= 2241 \text{ kbar}^{10)} \\ G &= 368 \text{ kbar}^{10)} \\ E' &= 5.285^{11)} \\ G' &= 1.907^{11)} \end{aligned} \tag{26}$$

and therefore:

$$\begin{aligned} E'/E &= 0.00236 \text{ kbar}^{-1} \\ G'/G &= 0.0022 \text{ kbar}^{-1} \end{aligned} \tag{27}$$

Thus, independent of the model for flow, ξ is expected to be about 0.002, as long as the flow stress is predominantly controlled by the pressure dependence of the elastic constants.

Experimentally, one finds that the critical shear stress of Fe single crystals varies with pressure[12] as $\xi = 0.0065$ kbar^{-1}. Measurements on polycrystalline Fe yield $\xi = 0.0048$ in the Lüdersband regime and $\xi = 0.0021$ kbar^{-1} in the uniform deformation, i.e., well deformed, regime[13]. The latter value corresponds closely to elastic constant case. Metallic glasses can be viewed as crystalline solids with a high enough dislocation content ($\sim 10^{14}$/cm^2) to destroy the long range order. From this point of view one would expect that their pressure dependence corresponds most closely to that of highly deformed crystals.

Amorphous $Fe_{40}Ni_{40}P_{14}B_6$ has Young's modulus of 1310 kbar[14], or about 60% of Fe. Assuming that E' is similar to the crystalline case, which is not unreasonable since the dimensionless quantity C_o' varies relatively little from material to material and lies generally between 2 and 6[9], the pressure dependence as described by ξ is calculated to be:

$$\xi = 0.00403 \text{ kbar}^{-1} \tag{28}$$

a value which is, undoubtedly somewhat fortuitously, very close to the measured value. However, the estimate serves to show that from the crystalline point of view, there is nothing unusual about the pressure dependence of the yield stress of a metallic glass. Models which analyze the flow of metallic glasses in terms of dislocations[15,16] are therefore compatible with the present result. Flow models based on free volume theory predict that the flow stress should vary with pressure as B'/B, where B is the bulk modulus[17]. Since the bulk modulus of metallic glasses is very similar to crystalline materials[18], an estimate along the above lines with $B' = 5$ yields a lower value of $\xi \approx 0.025$. However, given

the experimental error limits on ξ, and the uncertainties on how to estimate C_o', one must conclude that both approaches can account for the observed value of 0.0039. Precise measurements of the elastic constants and their pressure dependence would allow to discriminate between the two models.

Summary

The metallic glass $Fe_{40}Ni_{40}P_{14}B_6$ was deformed at pressures up to 250 kbar and strains in excess of 20% in a diamond anvil cell. The radial pressure distribution in the cell was measured with the fluorescent ruby R_1 line method to ± 1 kbar. An analysis of the measured pressure distribution indicates a critical shear stress of 8.5 kbar and a pressure coefficient of the critical shear stress of 0.0039. The critical shear stress is about 30% lower than the one measured with conventional methods. The decrease is ascribed to work softening, and a work softening coefficient $d\sigma/d\varepsilon \lesssim 1.5$ is derived. The pressure coefficient is similar to that of a PdSi base metallic glass and crystalline metals.

Acknowledgement

This research was sponsored by the Office of Naval Research under contract NR 039-151/N00014-77-C-0546 and supported by additional funds from the Materials Science Center at Cornell and National Science Foundation Grants EAR79-19978 and EAR78-04388.

References

1) L.A. Davis and S. Kavesh, J. Mat. Sci. 10 (1975) 453.

2) N. Polakowski and E.J. Ripling, "Strength and Structure of Engineering Materials", (Prentice Hall, N.Y., 1966) p. 300 ff.

3) N.P. Suh and A.P.L. Turner, "Elements of the Mechanical Behavior of Solids", (McGraw-Hill, N.Y., 1975) p. 521.

4) C.-M. Sung and C. Goetze, Rev. Sci. Inst. 48 (1977) 1386.

5) J.D. Barnett, S. Block and G.J. Piermarini, Rev. Sci. Instr. 44 (1973) 1.

6) D.J. Krenitsky and D.G. Ast, J. Mat. Sci. 14 (1979) 275.

7) D.G. Ast and D.J. Krenitsky, J. Mat. Sci.

8) D.E. Polk and D. Turnbull, Acta. Met. 20 (1972) 493.

9) J.O. Chua and A.L. Ruoff, J. Appl. Phys. 46 (1975) 4659.

10) J.A. Rayne and B.S. Chandrasekhar, Phys. Rev. 122 (1961) 1714.

11) C.A. Rotter and C.S. Smith, J. Phys. Chem. Sol. 27 (1966) 267.

12) W.A. Spitzig, Acta Met. 27 (1979) 523.

13) A. Oguchi, S. Yoshida and M. Nobuki, Trans. Jap. Inst. Met. 13 (.972) 63.

14) B. Berry, private communication.

15) J.J. Gilman, J. Appl. Phys. 44 (1973) 675.

16) J.C.M. Li, "Distinguished Lectures in Materials Science", (Marcel-Dekker, N.Y., 1974).

17) F. Spaepen and D. Turnbull, Scripta, Met. 8 (1974) 563.

18) J.J. Gilman, J. Appl. Phys. 46 (1975) 1625.

Figure Captions

Fig. 1 Diamond pressure cell.

Fig. 2 Measured pressure distribution of $Fe_{40}Ni_{40}P_{14}B_6$.

Fig. 3 Cross sectional view of specimen after loading.

Fig. 4 Measured pressure distribution of $Fe_{40}Ni_{40}P_{14}B_6$ after 2 step loading.

Fig. 5 Comparison of experimental data of Fig. 2 with prediction of eq. 21 τ=8.5 Kbar; § = 0.0039.

Fig. 6 Comparison of experimental data of Fig. 2 with prediction of eq. 21 τ=10.5 Kbar; § = 0.0039.

Fig. 7 Decomposition of experimental data of Fig. 4 into slipping and sticking regimes. (For details see text).

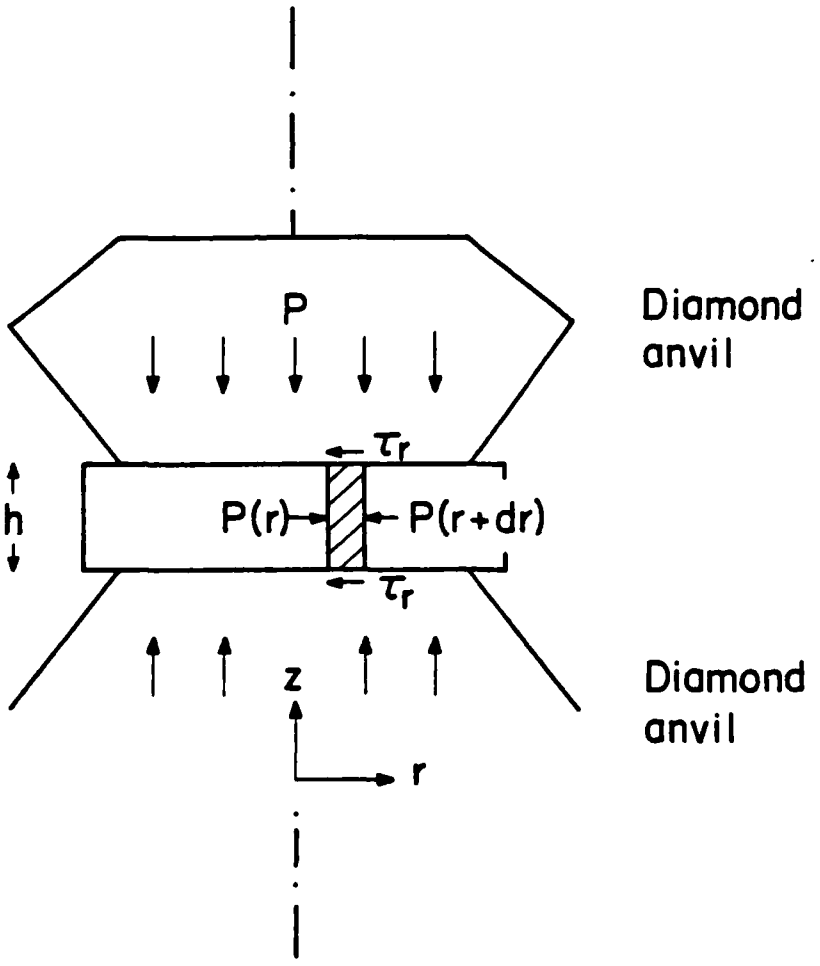
P
Diamond anvil
τ_r
h
P(r)
P(r+dr)
τ_r
z
r
Diamond anvil

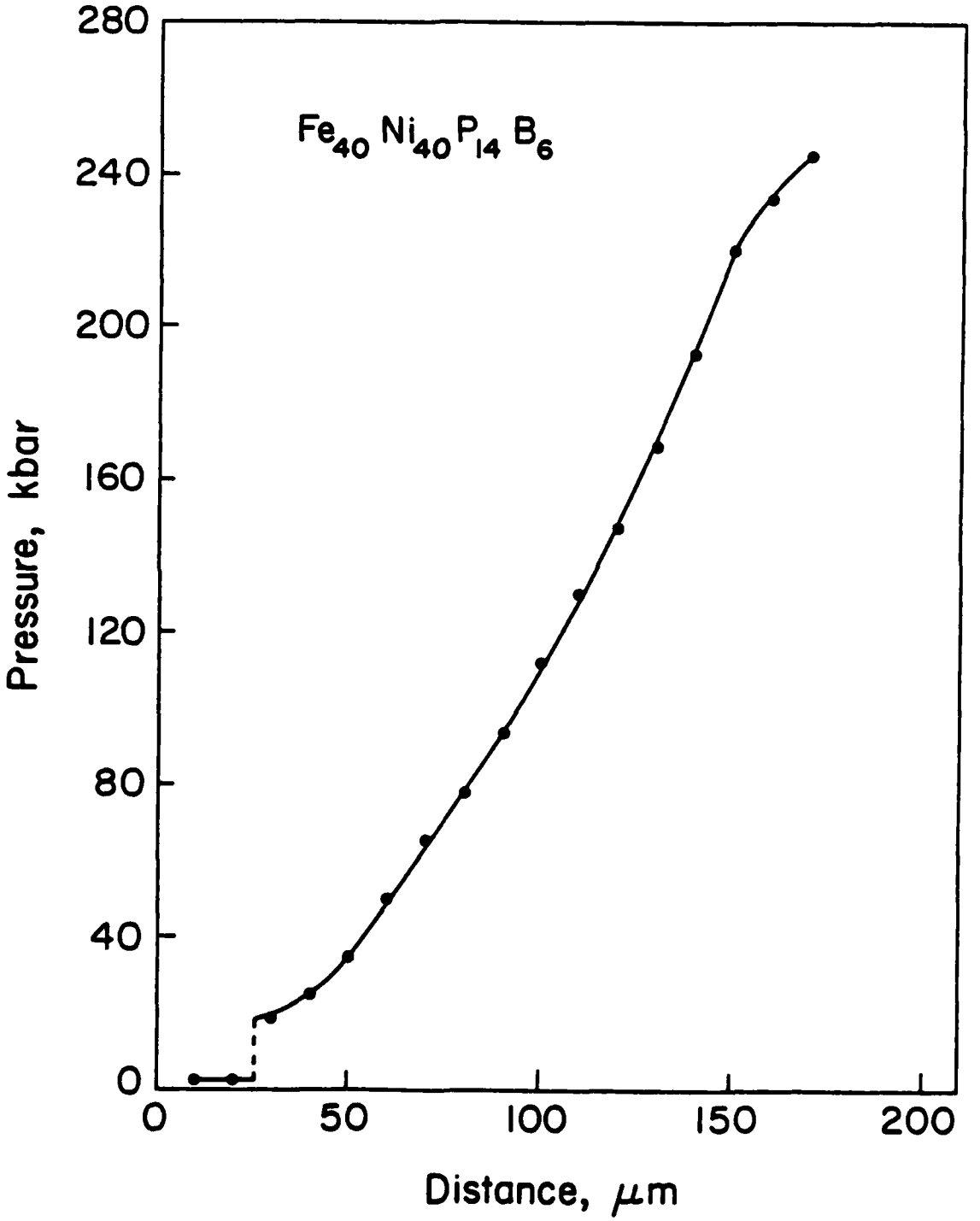
$Fe_{40}Ni_{40}P_{14}B_6$
Pressure, kbar
280
240
200
160
120
80
40
0
0
50
100
150
200
Distance, μm

Figure 2

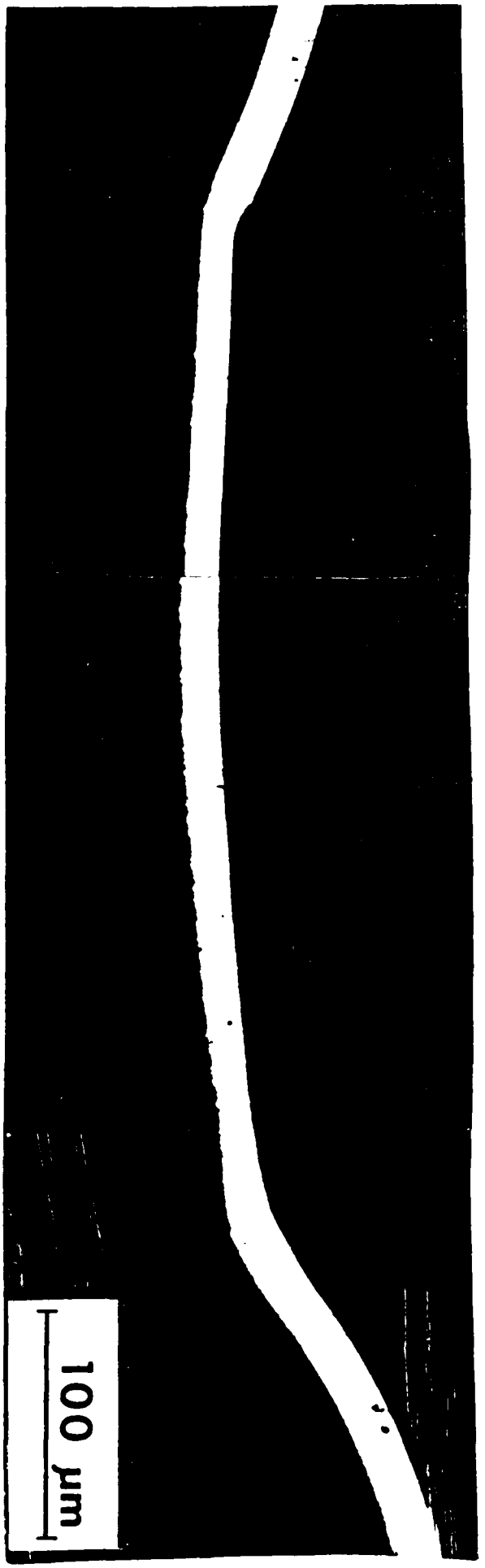

Figure 3

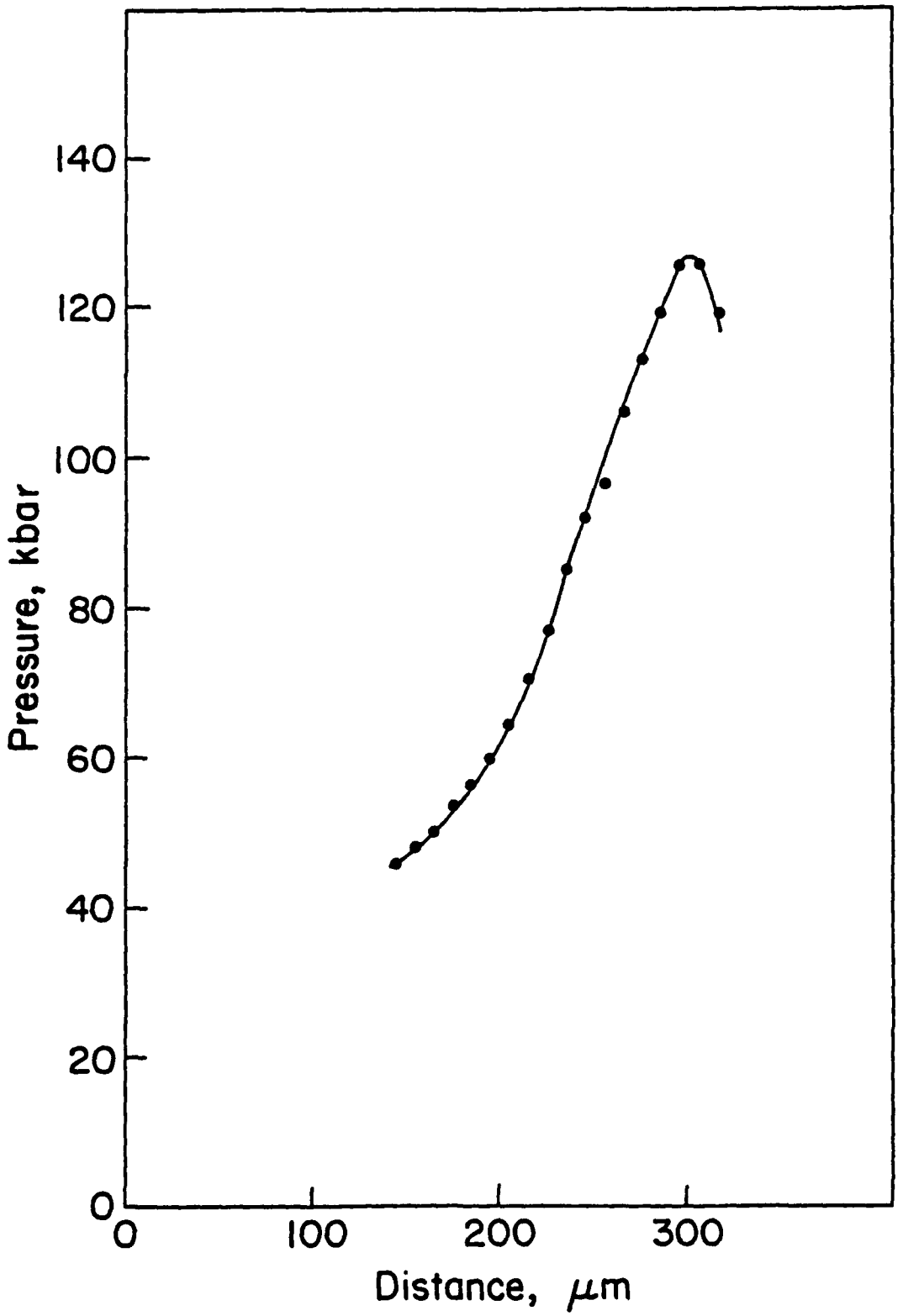
140
120
100
80
60
40
20
0
Pressure, kbar
0
100
200
300
Distance, μm

Figure 4

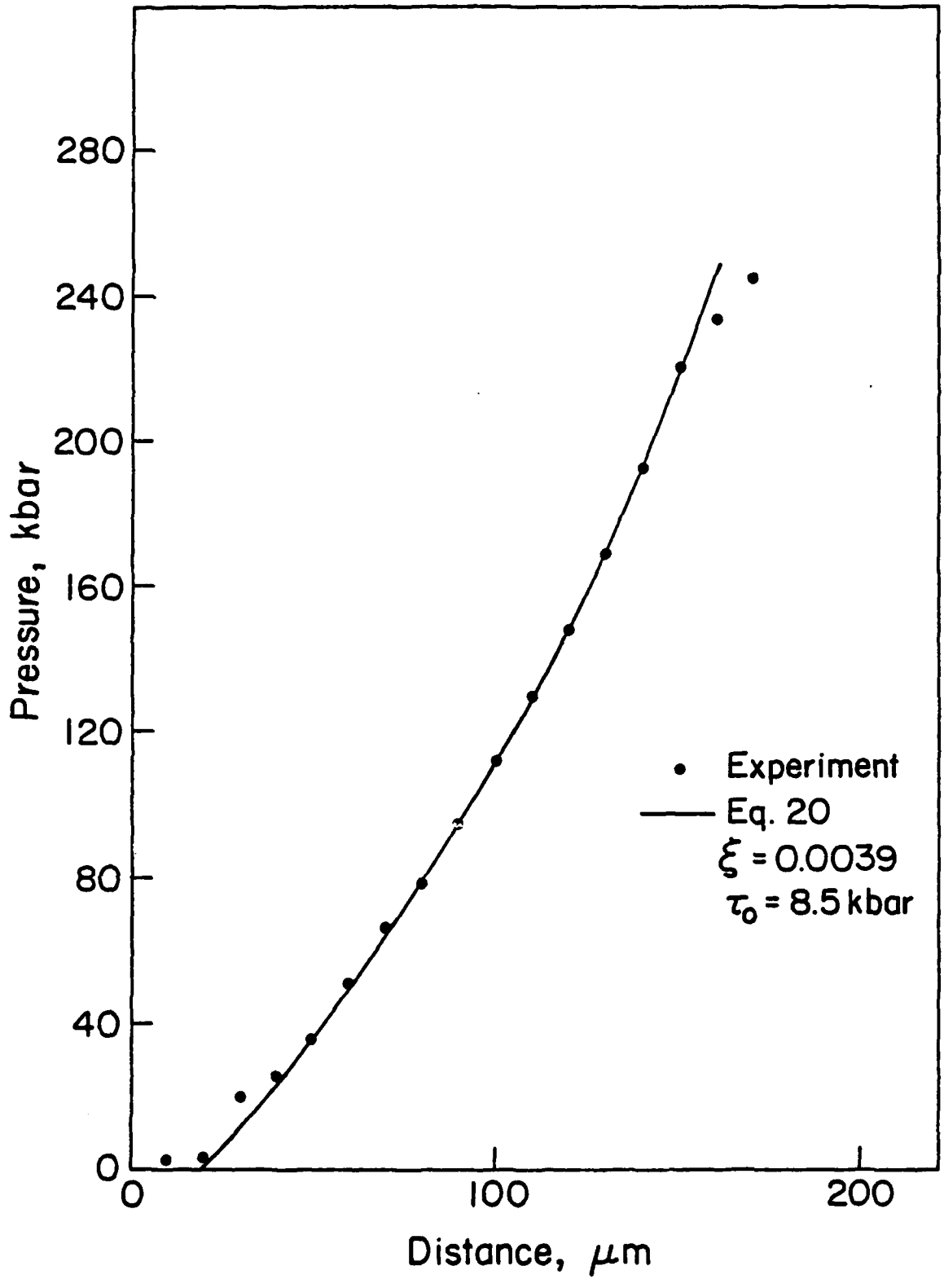
280
240
200
160
120
80
40
0
Pressure, kbar
0
100
200
Distance, μm
Experiment
Eq. 20
ξ = 0.0039
τ0 = 8.5 kbar

Figure 5

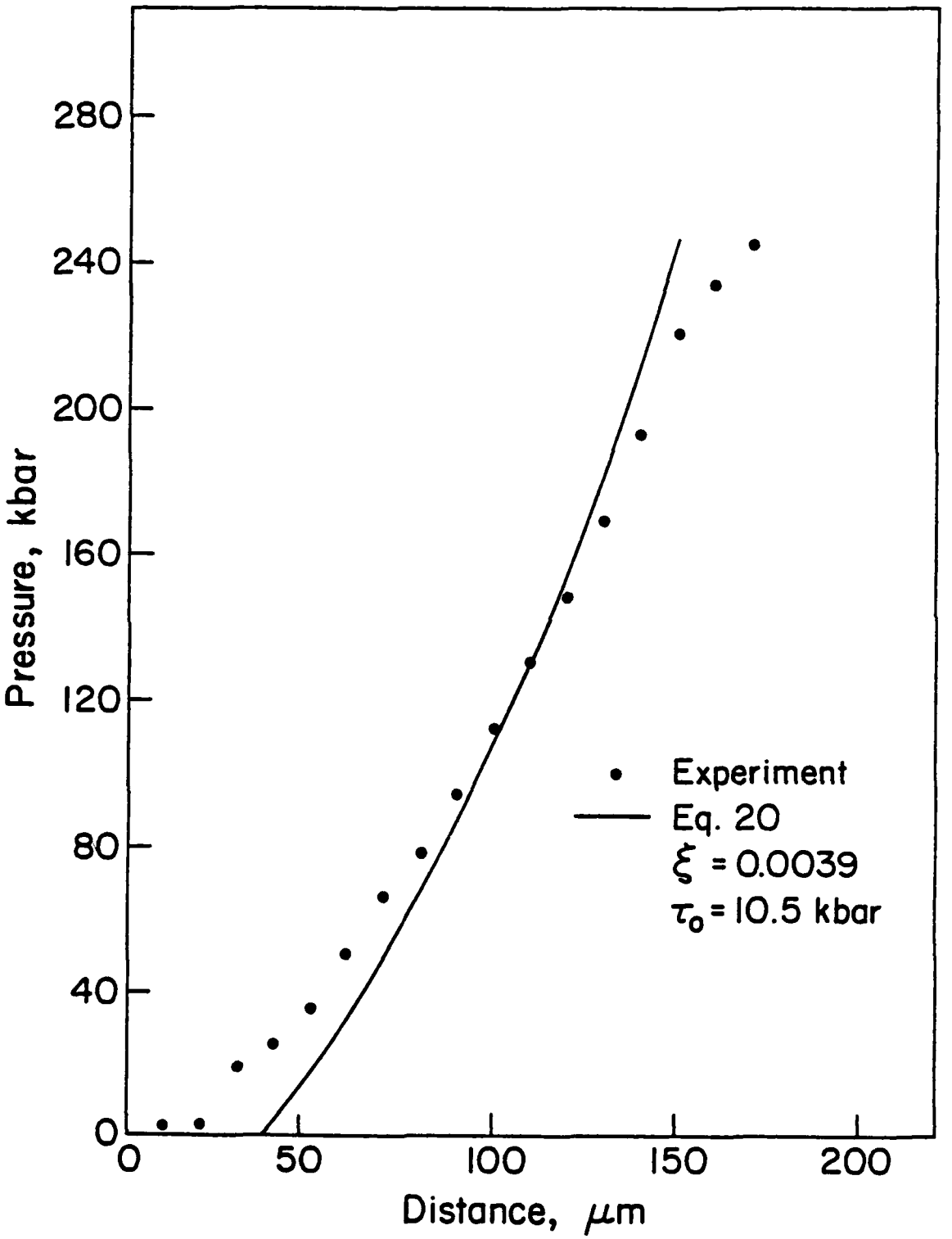
280
240
200
160
120
80
40
0
Pressure, kbar
0
50
100
150
200
Distance, μm
Experiment
Eq. 20
ξ = 0.0039
τ0 = 10.5 kbar

Figure 6

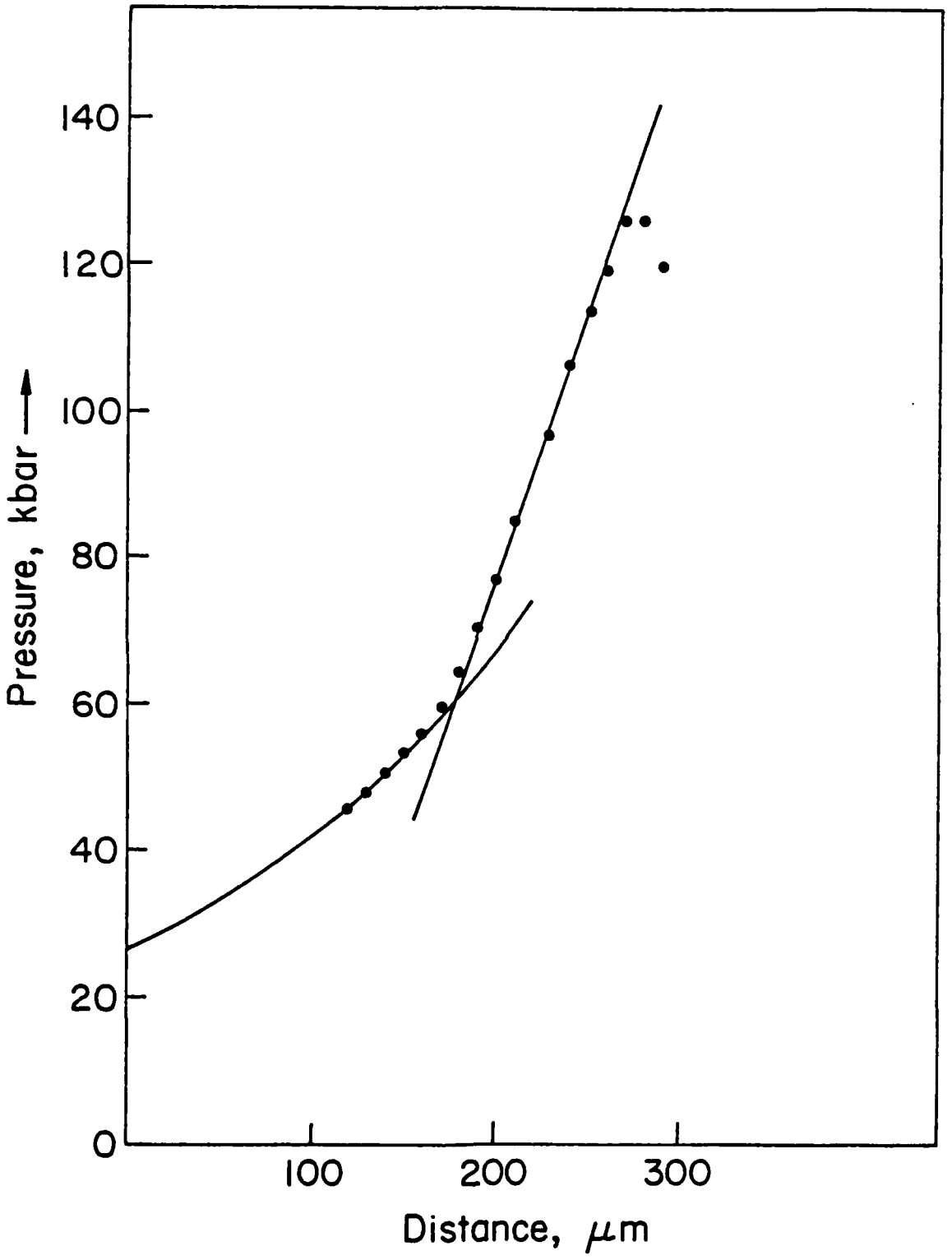

Figure 7

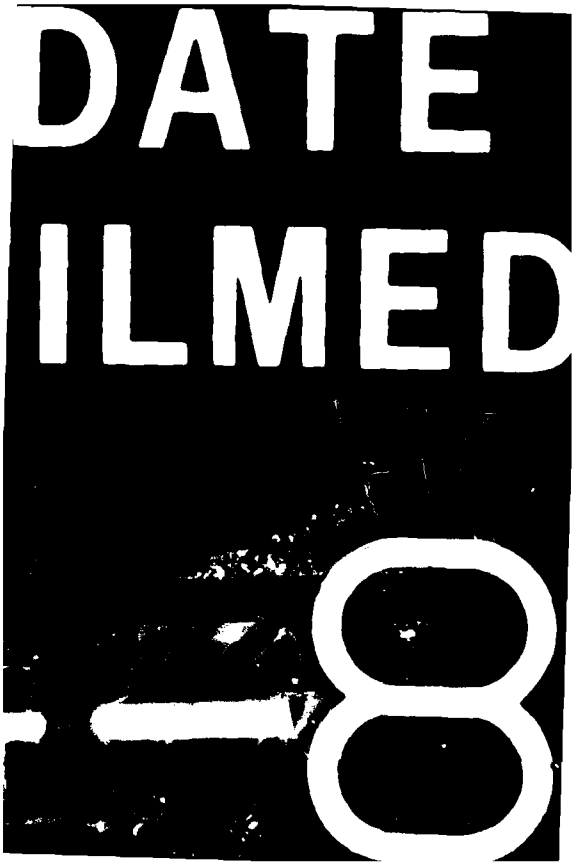
DATE
ILMED
8